

## RESEARCH ARTICLE

# Inflammatory state of lymphatic vessels and miRNA profiles associated with relapse in ovarian cancer patients

Sarah C. Johnson<sup>1</sup>, Sanjukta Chakraborty<sup>2</sup>, Anastasios Drosou<sup>3</sup>, Paula Cunnea<sup>4</sup>, Dimitrios Tzovaras<sup>3</sup>, Katherine Nixon<sup>4</sup>, David C. Zawieja<sup>2</sup>, Mariappan Muthuchamy<sup>2</sup>, Christina Fotopoulou<sup>4†</sup>, James E. Moore Jr.<sup>1†\*</sup>

**1** Department of Bioengineering, Imperial College London, London, United Kingdom, **2** College of Medicine, Texas A&M University, TX, United States of America, **3** Information Technologies Institute Centre for Research & Technology Hellas, Thessaloniki, Greece, **4** Department of Surgery and Cancer, Imperial College London, London, United Kingdom

† These authors are joint senior authors on this work.

\* [james.moore.jr@imperial.ac.uk](mailto:james.moore.jr@imperial.ac.uk)



## OPEN ACCESS

**Citation:** Johnson SC, Chakraborty S, Drosou A, Cunnea P, Tzovaras D, Nixon K, et al. (2020) Inflammatory state of lymphatic vessels and miRNA profiles associated with relapse in ovarian cancer patients. PLoS ONE 15(7): e0230092. <https://doi.org/10.1371/journal.pone.0230092>

**Editor:** Bernard Mari, Institut de Pharmacologie Moléculaire et Cellulaire, FRANCE

**Received:** February 20, 2020

**Accepted:** July 5, 2020

**Published:** July 27, 2020

**Copyright:** © 2020 Johnson et al. This is an open access article distributed under the terms of the [Creative Commons Attribution License](https://creativecommons.org/licenses/by/4.0/), which permits unrestricted use, distribution, and reproduction in any medium, provided the original author and source are credited.

**Data Availability Statement:** Further analytical results are available in the supplementary material. All raw and normalised expression data files have been deposited within NCBI's Gene Expression Omnibus and are accessible through GEO Series accession number GSE153719 (<https://www.ncbi.nlm.nih.gov/geo/query/acc.cgi?acc=GSE153719>).

**Funding:** CF and PC are funded by the Myrovlytis Trust (<https://www.myrovlytistrust.org/>), Rosetrees Trust (<https://rosetreestrust.co.uk/>) and Imperial Health Charity (<https://www.imperialcharity.org.uk/>)

## Abstract

Lymphogenic spread is associated with poor prognosis in epithelial ovarian cancer (EOC), yet little is known regarding roles of non-peri-tumoural lymphatic vessels (LVs) outside the tumour microenvironment that may impact relapse. The aim of this feasibility study was to assess whether inflammatory status of the LVs and/or changes in the miRNA profile of the LVs have potential prognostic and predictive value for overall outcome and risk of relapse. Samples of macroscopically normal human lymph LVs (n = 10) were isolated from the external iliac vessels draining the pelvic region of patients undergoing debulking surgery. This was followed by quantification of the inflammatory state (low, medium and high) and presence of cancer-infiltration of each LV using immunohistochemistry. LV miRNA expression profiling was also performed, and analysed in the context of high versus low inflammation, and cancer-infiltrated versus non-cancer-infiltrated. Results were correlated with clinical outcome data including relapse with an average follow-up time of 13.3 months. The presence of a high degree of inflammation correlated significantly with patient relapse ( $p = 0.033$ ). Cancer-infiltrated LVs showed a moderate but non-significant association with relapse ( $p = 0.07$ ). Differential miRNA profiles were identified in cancer-infiltrated LVs and those with high versus low inflammation. In particular, several members of the let-7 family were consistently down-regulated in highly inflamed LVs ( $>1.8$ -fold,  $p < 0.05$ ) compared to the less inflamed ones. Down-regulation of the let-7 family appears to be associated with inflammation, but whether inflammation contributes to or is an effect of cancer-infiltration requires further investigation.

), KN is funded by Imperial Private Healthcare (<https://imperialprivatehealthcare.co.uk/>) and Imperial Health Charity. DZ and JM acknowledge funding from NIH grant U01-HL123420. The funders had no role in study design, data collection and analysis, decision to publish, or preparation of the manuscript. The specific roles of all authors are articulated in the 'author contributions' section.

**Competing interests:** The authors have declared that no competing interests exist.

## Introduction

Epithelial Ovarian cancer (EOC) accounts for over 4000 deaths in the UK every year [1]. Lymph node (LN) metastases are very common in EOC-patients and associated with a more dismal overall prognosis [2,3]. Total macroscopic tumour clearance with removal of bulky LN is one of the most important prognostic factors for survival post-surgery in EOC [3,4]. There is no therapeutic value in the systematic removal of clinically normal appearing LN in the advanced disease setting, as shown in prospective randomised trials [5]. The involvement and changes in the connecting lymphatic vessels (LVs) and how they are related to the future risk of metastasis and relapse have never been investigated, to our knowledge.

LVs are specialised in the uptake and transport of macromolecules from tissue fluid, consequently permitting lymphogenic spread of cancer cells. Within the tumour microenvironment, intra-tumoural LVs are present, however functional tests in mice have indicated that intra-tumoural lymphatics are non-functional [6,7]. The collapse of intra-tumoural LVs is due to some combination of the high interstitial pressure observed in multiple types of tumours, a lack of lymphatic valves, or induced mechanical pressure of growing tumour cells [6]. However, in both mice and humans, functional peri-tumoural lymphatics remain [6]. LVs can facilitate metastases both passively and through active changes in lymphatic endothelial cell (LEC) expression that aid cancer-cell infiltration, allowing subsequent drainage to LNs [8]. Tumour cells can also arrest within the draining LVs and form in-transit metastases, and in some cases escape the LVs, contributing to loco-regional metastasis, potentially aided by altered LV barrier integrity [8].

Lymphatic endothelial cells (LECs) that line the LVs can also modulate immune cell function, in both anti-tumour immune response and cancer-induced immunosuppression [9]. For example, LEC expression of Protein-Death-Ligand 1 (PD-L1), the ligand for T cell inhibitory receptor, PD-1, can contribute to peripheral tolerance in LNs and tumours [10]. Tumour associated LECs can scavenge and cross-present tumour-antigen to cognate CD8<sup>+</sup> T cells, displaying the ability to endogenise allergen ovalbumin, then present the exogenous antigen on Major Histocompatibility Complex (MHC) class I molecules, and contribute to inducing tolerance of tumour-specific CD8<sup>+</sup> T cells [11]. LECs of the LN can acquire peptide MHCII-from dendritic cells and induce tolerance of CD4<sup>+</sup> T cells via subsequent presentation, in addition to up-regulating MHCII in response to viral-induced inflammation or Interferon-gamma (IFN- $\gamma$ ) [12]. LVs are also sensitive to inflammation-induced signalling molecules which can promote lymphangiogenesis, and induce further secretion of inflammatory molecules that may drain to the LNs [13]. Chronic inflammation in collecting LVs induce changes including LV dilation and inhibition of contractile ability but the effects on metastasis are unknown [14].

MicroRNAs provide vital post-transcriptional regulation of gene expression, a function that is often disrupted by cancer [15]. The ability of a single miRNA to inhibit multiple target genes has led to several studies of altered tumour miRNA expression in ovarian cancer and response to chemotherapy. This includes comparison of miRNA expression in different tumour subsets, in healthy versus diseased ovaries, in patient versus healthy serum, benign versus malignant tumours, expression associated with reduced patient survival, and expression associated with drug-resistance [16]. For example, a study using both EOC cell lines and EOC tumour tissue showed highly elevated miR-221, decreased miR-21 expression, and down-regulation of several members of the let-7 family [17].

Expression of miRNAs in LVs and LECs is altered during inflammation and by nearby tumours. In inflamed LECs, upregulated miR-1236 reduced expression of vascular-endothelial growth factor-3 receptor, inhibiting lymphangiogenesis [18]. A separate study showed that inflamed dermal LECs increased miR-155 expression, a miRNA with known involvement in

PD-L1 expression which may contribute to peripheral tolerance changes [19]. Furthermore, a panel of differentially expressed miRNAs was identified in inflamed rat LECs and human LEC culture, indicating effects on inflammation, angiogenesis, endothelial mesenchymal transition, cell proliferation and senescence pathways [13]. Tumour expression profiling has identified changes in lymphangiogenesis-inducing miRNAs, such as miR-126 in oral cancer and miR-128 in non-small cell lung cancer, that could influence metastasis [20,21]. A study using human LEC co-culture models of gastric cancer, representing tumoural or draining LVs, identified changes in differential miRNA expression associated with lymphangiogenesis and with positive lymphatic metastasis [22]. Further miRNA expression studies of draining LVs are lacking but many gene dysregulations were identified in LECs isolated from afferent LVs that drained a metastatic gastric tumour in rats, including up-regulation of chemokine CXCL1 [23].

The aim of this feasibility study was to provide insight into, and assess the prognostic value of the changes in the inflammatory state and miRNA expression of the transporting LVs in EOC. It is expected that these changes will be indicative of the immune response in the LVs and the downstream LN, and therefore could be predictive of patient prognosis.

## Methods

### LV sample collection

LVs were collected from patients undergoing debulking surgery for advanced stage (FIGO IIC, III or IV) epithelial ovarian cancer at Hammersmith Hospital, Imperial College Healthcare NHS Trust, London, United Kingdom (Table 1 and S1 Table). Informed consent was provided from each patient. Ethics committee approval was obtained from Hammersmith and Queen Charlotte's and Chelsea Research Ethics Committee (REC reference: 05/Q0406/178), and tissue samples were provided by the Imperial College Healthcare NHS Trust Tissue Bank (ICHTB). The following LV processing steps are summarised in S1 Fig.

**Table 1. Summary of the LV microscopic state and clinical data.**

Vessel Sample	Type of marker			Stage	Histology	LN histology	Relapse (mos)*
	MPO	WT1	Pax-8				
1	+++	+++	++	IVB	HGS	N0	y(11)
2	+++	+++	+++	IVA	HGS	Nx	y(12)
3	+++	-	-	IIC	HGS	Nx	y(13)
4	+	++	+	IV	HGS	Nx	y(9)
5	-	-	-	IIIB	CC	Nx	n
6	-	-	-	IIIC	HGS	Nx	n
7	-	-	-	IIIC	HGS	N1	n
8	-	-	-	IIIC	HGS	Nx	n
9	+	-	-	IVB	HGS	Nx	n
10	+	+	++	IIC	HGS	N0	n
Key	MPO	WT1/Pax-8		Histology		LN histology	
	+++ high	+++ = 15 cells		HGS = high grade serous		N0 = Negative status	
	+ medium	++ 15 > cells > = 5		CC = clear cell carcinoma		N1 = Positive status	
	- low	+ < 5 cells				Nx = Unassessed status	

Sections of the LVs were stained with antibodies for the inflammatory marker myeloperoxidase (MPO), ovarian cancer markers Wilms-Tumour-1 (WT1) and Paired Box Gene 8 (Pax-8), and the lymphatic endothelial marker, Podoplanin (PDPN).

\*Mean time since surgery = 13.2 ± 3.6 months.

<https://doi.org/10.1371/journal.pone.0230092.t001>

Macroscopically normal appearing LVs along the external iliac vessels with surrounding fibro-fatty tissue were removed with the nearby LN as part of the debulking procedure. Vessels were ligated with VICyl03 or PDS-4-0, avoiding bipolar coagulation and other thermic energy to limit vessel damage. All patients had no macroscopic residual disease after surgery.

### Vessel isolation and storage

Tissue specimens were transported directly from surgical theatre to the laboratory in ice-cold sterile Phosphate Buffered Saline (VWR, UK). LVs were identified and isolated along with a small amount of surrounding tissue under a dissection microscope within a sterile laminar flow cabinet (Fig 1A–1C). Each vessel was divided into two sections. One half of each vessel was further cleaned of surrounding fatty tissue, placed in RNA stabilising solution (RNAlater, ThermoFisher, UK), frozen on dry ice and stored at  $-20^{\circ}\text{C}$ . The other half was fixed in 4% paraformaldehyde (VWR, UK) for 45 minutes, followed by submersion in 15% sucrose for 3 hours, then 30% sucrose for 6–12 hours. This was followed by embedding in OCT (Scigen, UK) using dry ice and isopropyl alcohol (ThermoFisher, UK) and stored at  $-80^{\circ}\text{C}$ .

### MiRNA extraction and analysis

Samples in RNAlater were individually defrosted and homogenized in 700 $\mu\text{L}$  of QIAzol (Qiagen, UK), using a PT 1300 D homogeniser with a 3mm dispersing aggregate head (Kinematica, Switzerland) at 20,000 RPM in a sterile 1.5 ml tube. RNA was extracted using a miRNeasy Mini Kit (Qiagen, UK) following the standard protocol and quality was verified using a NanoDrop<sup>TM</sup> 2000 at A260/280nm and A260/230nm absorbance (ThermoFisher, UK). Each sample was reverse-transcribed to cDNA using a miScript II RT Kit (Qiagen), then qPCR was carried out using a miScriptSybrGreen real-time PCR kit (Qiagen) and pre-defined miScript miRNA PCR Array (Qiagen, UK). The array contained primer pairs for 8 housekeeping genes and controls plus 88 human miRNAs that have previously been identified or predicted to

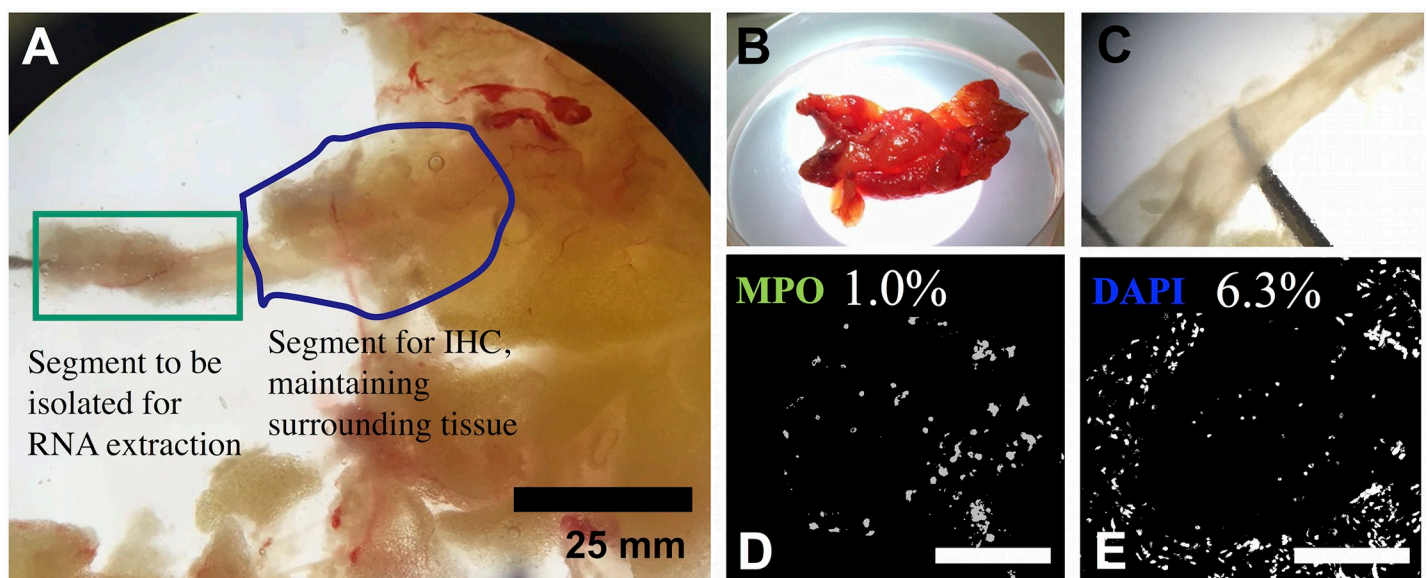


**Fig 1. Lymphatic vessel isolation and classification.** A. LV isolation technique. B. Tissue sample containing LV. C. Isolated and cleaned vessel for RNA extraction. D&E, Quantification of LVs inflammation was determined using the ratio of MPO staining to cell nuclei (DAPI), in this example  $1.0\%/6.3\% = 0.16$ , to divide samples into low, medium and high inflammatory states with thresholds of  $<3\%$ ,  $3\text{--}10\%$  and  $>10\%$  respectively.

<https://doi.org/10.1371/journal.pone.0230092.g001>

target genes involved in the regulation of inflammatory responses and autoimmunity. One well was populated with a negative control sample. The array was run using a StepOnePlus Real-Time PCR System (Applied Biosystems), according to the manufacturer's instructions.

### Immunofluorescence staining and imaging

Samples embedded in OCT were sectioned at 10–16 $\mu$ m and stored at -80°C. Both standard Haematoxylin and Eosin (H&E) and immunofluorescent staining were subsequently performed. For immunofluorescent staining, slides were washed with Tris Buffered Saline (TBS) (Sigma-Aldrich, UK) and 0.05% Triton-X (Sigma) and blocked for 1 hour with 10% goat serum/TBS (Sigma-Aldrich). Slides were incubated overnight at 4°C with primary antibodies diluted in 5% goat serum/TBS at ratios of 1:200 for inflammatory marker Myeloperoxidase (MPO) (ab9535), 1:200 for ovarian carcinoma marker Wilms Tumour-1 (WT1) (ab89901), 1:50 for ovarian carcinoma marker Paired-Box-Gene 8 (Pax-8) (ab189249), and 1:200 for LEC marker Podoplanin (PDPN) (ab10288). Alexa-488 conjugated secondary antibody, anti-Mouse (ab150113) or anti-Rabbit (ab150077) were applied at a dilution of 1:250 in 5% goat serum/TBS at room temperature for 1 hour. Samples were stained with DAPI (4',6-diamidino-2-phenylindole) solution (Sigma-Aldrich) and mounted with Fluoroshield (Sigma-Aldrich). Confocal Z-stacks and multi-channel images were processed and analysed using FIJI imaging software [24].

Assessment of H&E staining confirmed cryo-sections of LV samples stored at -80°C maintained sufficient morphology to quantify inflammation and cancer cell presence. The identification of LVs was confirmed by the positive staining with Podoplanin. The LV were subsequently classified into a low, medium or high inflammatory group with thresholds of <3%, 3–10% and >10% of MPO staining to nuclei (DAPI) staining ratio (Fig 1D and 1E). The level of cancer-cell infiltration was determined by the number of cancer cells detected in a LV cross-section, as shown by positive staining with WT1 and Pax-8.

### Statistical analysis

Clinical correlation between different combinations of LV state (inflammation, high-inflammation, cancer-infiltration), and patient relapse, and cancer-stage were assessed by applying Fishers exact test, to identify significant non-random associations, and calculation of Cohen's Kappa coefficient of inner agreement ( $\kappa$ ), interpreted according to the methods of Vierra and Garrett 2005 [25]. A P value below 0.05 was considered statistically significant. Kaplan Meier estimates of probability of non-relapse were also calculated for cancer-infiltration, inflammation and age. Prior to further analysis, the miRNA expression of each LV ( $\Delta$ CT) was normalized to the expression of a stably expressed gene in each array, confirmed with NormFinder (<http://moma.dk/normfinder-software>) and GeNorm (<http://www.biogazelle.com/qbaseplus>) software. SNORD96 was selected as a reference "housekeeping" gene. The fold change between imaging-informed groups of LVs was calculated as  $\Delta\Delta$ CT Group2/ $\Delta\Delta$ CT Group1 where  $\Delta\Delta$ CT =  $2^{\Delta$ CT. Fold regulation was normalised to values greater than 1, noting up- or down-regulation. Principle component analysis (PCA) was used to transform multivariate data linearly into a set of uncorrelated variables to identify patterns in the variance amongst the data. We applied PCA to the miRNA expression recorded across all our samples to calculate two principle components (PC) that account for the greatest sources of miRNA variation within samples, using online software ClustVis (<https://biit.cs.ut.ee/clustvis/>) [26]. In cases where more than 1 miRNA was identified as significantly up-regulated or significantly down-regulated, pathway analysis was carried out using Diana-MiRPath v3 [27]. After removing miRNA that did not show a >1.8 fold-regulation change, a student-t-test, assuming equal variance,

was applied to further confirm variation between groups. To visualise the distributions of the individual miRNA for which statistical significant difference was identified between groups, the probability density functions for miRNA expression in each group were estimated using Kernel Density Estimated distributions.

A number of widely used automatic classification methods were then used to predict the binary outcomes of the individuals (relapse vs. non-relapse, cancer infiltration vs. no cancer infiltration, medium or inflammation versus low inflammation), based on the LV miRNA expression of the individuals as predictor (input) variables. We used the supervised classification methods Logistic Regression, K-Nearest Neighbours, Support Vector Machine, Random Forest, and Gaussian Naïve Bayes. Evaluation of each method was performed using a leave-one-out cross validation procedure: each patient was considered in turn as a new patient (i.e. the test patient), while the remainder were considered as the training set. The predicted and actual outcome for each test patient was then compared with method accuracy measured as the percentage of correct predictions. Two other measures of accuracy were also used: the Cohen's Kappa coefficient ( $\kappa$ ) of inner agreement between predicted and actual values, and the McNemar's test measuring the significance of equality of predicted probability (inner accuracy) between groups for each outcome. In each method, we also split the cases according to the binary outcome variable and measured the percentage of correct predictions in each group. A set of only the miRNA that were significantly differentially expressed between groups was then used to train new classifiers. We then assessed whether use of the new classifiers could improve predictions when compared to the performance of classifiers built using the entire miRNA expression set.

## Results

### Post-operative assessment of patients

Ten patients were included in the present analysis. Nine of those patients had a high grade serous histology, and one patient had a clear cell carcinoma (Table 1). 60% of the lymph vessels were harvested at primary debulking surgery and 40% at interval debulking surgery (S1 Table). Only one positive para-aortic LN was detected at final histopathology. In the  $13.2 \pm 3.6$  months follow up period, 4 of the 10 patients had relapsed. Of the four patients that relapsed, three vessels demonstrated high inflammation and one vessel showed medium inflammation. Vessels from patients that did not relapse showed low inflammation in 4 cases and medium inflammation in the remaining 2 cases. Of the four relapse cases, cancer-cell infiltration was detected in three vessels (two with high inflammation and one showing medium inflammation). The overall relative range of inflammation in the lymphatic vessels was small with high inflammation defined as an average of  $>10\%$  MPO:DAPI ratio and a narrow range of an average of 3–10% MPO:DAPI ratio for medium inflammation. All vessels showed less inflammation than similarly stained ovarian tumour tissue (Fig 2I). Consequently, to compare LVs with a notable difference in inflammation we focused initially on comparison of the LVs with high inflammation versus low inflammation.

### Clinical correlation of LV inflammatory state or cancer-cell infiltration and patient relapse

Of the four cancer-infiltrated LVs identified, 2 presented with high inflammation and the remaining 2 samples presented with medium inflammation. Cancer-free LVs presented with generally lower degrees of inflammation (Table 1). Tumour cells were detected in 50% of LVs with medium inflammation and two-thirds of LVs displaying high inflammation. The LVs

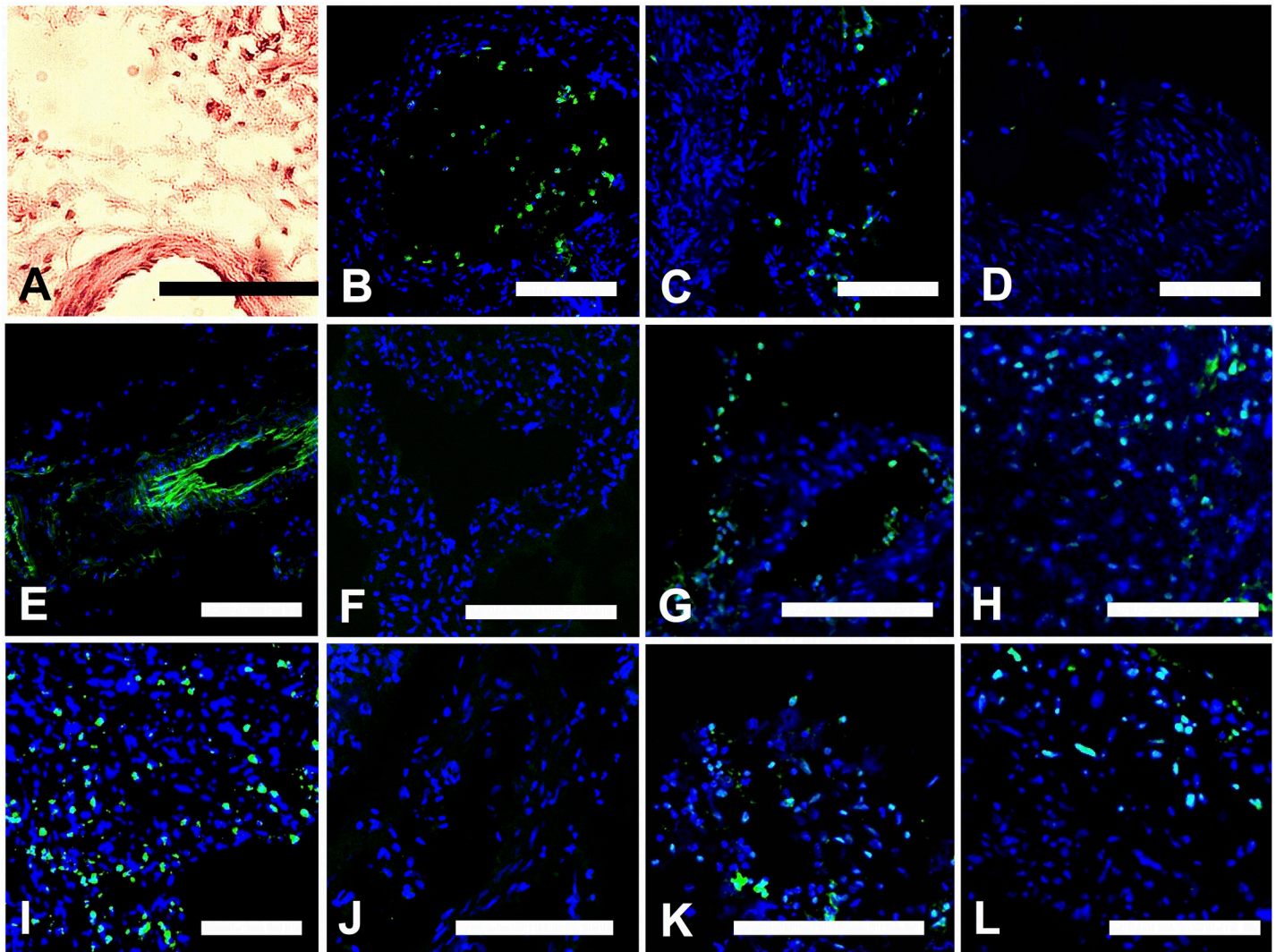


**Fig 2. Lymphatic vessel imaging.** A. H & E stained sections of the LVs, show that the nuclei were sufficiently preserved for subsequent Paired-Box-Gene 8 (Pax-8) and WT1 (Wilms-Tumour-1) staining. B-D. LVs with high, medium and low/no inflammatory state determined with myeloperoxidase (MPO) staining. E. Confirmation of LV status was carried out using LEC marker Podoplanin (PDPN) that stained around the LV lumen. F-H. Imaging with WT1, (F) negative LV, (G) positive LV (H) positive control. I. Tumour MPO positive control. J-L. Imaging with Pax-8, (J) negative LV, (K) positive LV and (L) positive control. An Ovarian tumour sample was used as a positive control and stained for both (M) WT1 and (Q) Pax-8. Scale = 140µm.

<https://doi.org/10.1371/journal.pone.0230092.g002>

presented with high inflammation in 3 of 10 samples, two of which were also positive for cancer cells. Three LV samples presented with medium inflammation, two of which contained cancer cells, and the remaining 4 LV samples presented with low inflammation and no detectable cancer cell infiltration (Table 1). The samples were macroscopically normal in appearance, however positive staining for the ovarian tumour markers WT1 and Pax8 was observed in four of the 10 samples collected (Fig 2G and 2K). The LVs with cancer cells showed a moderate agreement ( $\kappa = 0.583$ ) with patient relapse but this was not significant (Table 2) ( $p = 0.114$ ). A moderate but statistically non-significant agreement was found between cancer-infiltrated LVs and Stage IV and inflammation ( $\kappa = 0.583, 0.61$  respectively).

As the degree of inflammation in the LVs increased, so did correlation with patient relapse.

**Table 2. Cohen's Kappa Coefficient for inner-agreement between different sample states (1 = perfect agreement) and Fisher's exact test for identification of significant non-random association ( $p < 0.05$ ) (n = 10).**

Cohen's Kappa Co-efficient					
	Relapse*	Inflam.	High Inflam.	Cancer-cell inf.	Stage IV
Relapse	x	0.615	<b>0.783</b>	0.583	0.583
Inflam.	0.615	x	x	0.615	0.615
High Inflam.	<b>0.783</b>	x	x	0.348	0.348
Cancer-cell inf.	0.583	0.615	0.348	x	0.583
Stage IV	0.583	0.615	0.348	0.583	x
Fishers Exact Test (p-value)					
	Relapse*	Inflam.	High Inflam.	Cancer-cell inf.	Stage IV
Relapse	x	0.071	<b>0.033</b>	0.114	0.114
Inflam.	0.071	x	x	0.071	0.071
High Inflam.	<b>0.033</b>	x	x	0.3	0.3
Cancer-cell inf.	0.114	0.071	0.3	x	0.114
Stage IV	0.114	0.071	0.3	0.114	x

Inflam = comparison of LVs with high or medium inflammation to low inflammation. High Inflam. = comparison of LVs with high inflammation to low or medium inflammation. Cancer-cell inf. = cancer-cell infiltration.

\* Mean time since surgery = 13.2 months  $\pm$  3.6.

<https://doi.org/10.1371/journal.pone.0230092.t002>

The presence of LVs showing high inflammation significantly correlated with patient relapse ( $\kappa = 0.783$ ,  $p = 0.03$ ) (Table 3). The presence of medium or high inflammation within LVs showed a moderate agreement with patient relapse ( $\kappa = 0.615$ ,  $p = 0.07$ ) and patients with Stage IV, relapse and cancer-cell infiltration ( $\kappa = 0.615$ ,  $p = 0.07$ ) (Table 2). The presence of highly inflamed LVs compared to the presence of low inflammation only, resulted in a stronger correlation involving high inflammation status (Table 3). LVs exhibiting high degrees of inflammation showed near perfect agreement with patient relapse compared to those with low inflammatory state ( $n = 7$ ,  $\kappa = 1.0$ ,  $p = 0.029$ ). Additionally, there were indications of a relationship between highly inflamed vessels with cancer-infiltration and Stage IV cancer ( $\kappa = 0.695$ ), but this lacked statistical significance ( $p = 0.143$ ). These results therefore support the earlier identified correlation between high inflammation and relapse. Kaplan Meier estimates of non-relapse according to inflammatory state, cancer-infiltration and age thresholds ( $>55$ ,  $>60$ ,  $>70$ ,  $>75$  years) indicate that probability of non-relapse is decreased in patients with LVs displaying medium or low inflammation and patients with cancer-infiltrated LVs (S2 Fig). Probability of non-relapse showed that patients  $>55$  years age were more likely to relapse (S3 Fig).

## Lymphatic vessel miRNA expression during EOC

Expression analysis of a panel of miRNA involved in auto-immunity and inflammation was carried out. This showed that let-7 was differentially expressed in the highly-inflamed LVs

**Table 3. Comparison of LVs with high inflammation vs those with low inflammation only (n = 7) using Cohen's Kappa Coefficient and Fisher's exact test, as described in Table 2.**

	Relapse*	Cancer	Stage IV
Cohen's Kappa Co-efficient	<b>1</b>	0.695	0.695
Fishers Exact Test	<b>0.029</b>	0.143	0.143

\* Mean time since surgery = 13.2 months  $\pm$  3.6.

<https://doi.org/10.1371/journal.pone.0230092.t003>

Table 4. Differential expression of miRNA between LV groups displaying low, medium or high inflammation.

Low versus High			Low versus [Medium or High]		
miRNA	Fold regulation	t-test (p)	miRNA	Fold regulation	t-test (p)
let-7a-5p	-188.20	0.0389	let-7g-5p	-2.39	0.0308
let-7b-5p*	-11.42	0.0006	let-7i-5p	-2.02	0.0130
let-7c-5p*	-6.43	0.0003	miR-545-3p	-2.77	0.0739
let-7d-5p*	-5.06	0.0009	miR-93-5p	1.77	0.0856
let-7e-5p	-2.67	0.0802			
let-7f-5p	-3.20	0.0378			
let-7g-5p	-2.99	0.0969			
let-7i-5p	-2.23	0.0328			
miR-15b-5p	-5.24	0.0696			
miR-23a-3p	-3.44	0.0401			
miR-23b-3p	-15.17	0.0152			
miR-98-5p	-4.63	0.0823			

Listed are miRNA that showed a fold-change  $\pm 1.8$ , with subsequent t-test with  $p < 0.1$ , with miRNA displaying a significant difference of  $p < 0.05$  highlighted in bold.

\* = Bonferroni correction  $p < 0.0017$ .

<https://doi.org/10.1371/journal.pone.0230092.t004>

(Table 4, S2 Table). Significant differential expression of 8 miRNA was identified when comparing miRNA expression of LVs presenting with high inflammation versus low inflammation ( $p < 0.05$ ,  $n = 7$ ). Of the 8 miRNA, 6 belonged to the let-7 family with miR-23a-3p and miR-23b-3p completing the set. Differential expression can also be clearly visualised when the estimated probability density functions, calculated using kernel density estimation for inner groups, for the differentially expressed individual miRNA are compared (S4 Fig). Correction for multiple testing by applying a post-hoc Bonferroni correction showed that differential expression of three miRNA, let-7b, let-7c and let-7d remained significant ( $p < 0.0017$ ). Comparison of miRNA expression in LVs displaying low inflammation versus medium or high inflammation showed a similar trend towards down-regulation of the let-7 family (Table 4, S3 Table). Six miRNA were down-regulated  $> 1.8$  fold with significant down-regulation of let-7g-5p and let-7i-5p ( $p < 0.05$ ).

Similar trends were observed in the differential miRNA expression identified in the inflamed LVs and the differential miRNA expression in LVs collected from patients who underwent relapse during the study. Four significantly differentially expressed miRNA ( $p < 0.05$ ) were identified in relapse LVs (let-7c-5p, let-7b-5p, miR-23b-3p and miR-186-5p), with three of these (let-7c-5p, let-7b-5p, miR-23b-3p), also significantly differentially expressed in highly inflamed LVs (Table 5). Differential expression of miRNA with correction criteria of  $p < 0.002$  was not identified. Of the 17 miRNA that were down-regulated  $> 1.8$  fold in relapse vessels, 8 were also down-regulated in inflamed LVs, and 11 in the highly-inflamed LVs, including 5 and 6 members of the let-7 family respectively and miR-23b-3p (S2, S3 and S5 Tables).

In the cancer-infiltrated LVs, most miRNA expression changes involved miRNA up-regulation such as miR-16-5p, miR-93-5p and miR-497-5p, miR-381-3p, miR-144-3p and miR-181a-5p ( $p < 0.05$ ) (Table 5). Of these, up-regulation of miR-93-5p and miR-144-3p remained significant with application of a Bonferroni correction ( $p < 0.002$ ). In contrast, inflamed LVs presented with primarily down-regulated miRNA, in particular, significant down-regulation of members of the let-7 family along with miR-23a-3p, miR-23b-3p and tumour suppressor miR-15-5p [29]. In the cancer-containing LVs, only 7 miRNA showed a  $> 1.8$  fold down-

**Table 5. Differential expression of miRNA between cancer-infiltrated versus non-cancer infiltrated LVs and LVs from relapse versus non-relapse patients within 13.2±6 months.**

Cancer-infiltrated LVs			LVs from patients that relapsed		
miRNA	Fold regulation	t-test (p)	miRNA	Fold regulation	t-test (p)
<b>miR-144-3p*</b>	<b>14.02</b>	<b>0.0010</b>	miR-144-3p	5.07	0.0906
<b>miR-181c-5p</b>	<b>10.63</b>	<b>0.0170</b>	<b>miR-186-5p</b>	<b>4.93</b>	<b>0.0294</b>
miR-101-3p	5.08	0.0740	miR-497-5p	2.29	0.0672
<b>miR-381-3p</b>	<b>4.07</b>	<b>0.0140</b>	miR-34a-5p	2.09	0.0828
<b>miR-497-5p</b>	<b>2.9</b>	<b>0.0260</b>	miR-98-5p	-3.43	0.0673
<b>miR-93-5p*</b>	<b>2.25</b>	<b>0.0010</b>	let-7d-5p	-3.68	0.0645
<b>miR-16-5p</b>	<b>2.08</b>	<b>0.0310</b>	<b>let-7c-5p</b>	<b>-4.33</b>	<b>0.0385</b>
<b>let-7i-5p</b>	<b>-2.08</b>	<b>0.0210</b>	<b>let-7b-5p</b>	<b>-6.94</b>	<b>0.0383</b>
let-7b-5p	-2.27	0.0700	<b>miR-23b-3p</b>	<b>-8.53</b>	<b>0.0278</b>
let-7c-5p	-2.56	0.0780			

Listed are miRNA that showed a fold-change  $\pm 1.8$ , with subsequent t-test with  $p < 0.1$ , with miRNA displaying a significant difference of  $p < 0.05$  highlighted in bold.

\* = Bonferroni correction  $p < 0.002$ .

<https://doi.org/10.1371/journal.pone.0230092.t005>

regulation, 6 of which were members of the let-7 family (S4 Table). Of these six, five were also down-regulated  $> 1.8$ -fold in the LVs of patients who relapsed during the study period.

Similar trends in the differential miRNA expression in cancer-infiltrated LVs and highly inflamed LVs were also identified, as 15 miRNA were found to undergo an expression change of  $> 1.8$  fold (up- or down-regulated) in both of the comparisons (S2 and S4 Tables). Six of the 7 miRNA that were down-regulated in both groups belonged to the let-7 family. This common trend in the fold-regulation difference in the highly inflamed and cancer-infiltrated LVs may be reflective of the fact that 50% of the cancer-infiltrated LVs also presented with high inflammation. We also noted that the number of differentially expressed miRNA was higher when comparing LVs presenting with high or low inflammation than when comparing vessels with or without cancer-infiltration. Expression of several miRNA were consistently below qPCR detection levels and thus omitted from further analysis.

### Pathway analysis of miRNA found to be dysregulated in inflamed or cancer-infiltrated LVs

Pathway analysis indicated that significantly dysregulated miRNAs are involved in maintaining LV integrity. The 7 miRNAs that were significantly upregulated in cancer-infiltrated LVs, and the 7 miRNAs that were significantly down-regulated in inflamed LVs have known involvement in various pathways related to the TGF $\beta$ -pathway, fatty acid biosynthesis, proteoglycans in cancer, glycosaminoglycan synthesis and glycan biosynthesis as well as the extracellular matrix receptor interactions pathway and adherens junction pathway (Table 6). No significantly up-regulated miRNAs were identified in highly inflamed LVs and only one significantly down-regulated miRNA was identified in cancer-infiltrated LVs. Pathway analysis carried out with the 4 significantly dysregulated miRNAs in the relapse LVs showed a range of potential target pathways including adherens junction, ECM-receptor interactions and mucin type O-Glycan biosynthesis (S6 Table).

### Principle component analysis of miRNA expression in LV samples

PCA showed that differential miRNA expression identified in inflamed and cancer-infiltrated LVs could also be identified without grouping the samples. This can be seen when assessing

**Table 6. Pathway analysis using MiRNA that were significantly up-regulated in cancer-infiltrated LVs (left-hand side) and miRNA significantly down-regulated >1.8 fold (right-hand side) in highly inflamed LVs.**

Upregulated miRNA in cancer-infiltrated LVs				Down-regulated miRNA in highly inflamed LVs			
KEGG pathway	p-value	Genes	miRNA	KEGG pathway	p-value	Genes	miRNA
TARBASE				TARBASE			
Proteoglycans in cancer	3.02E-15	96	5	Adherens junction	5.86E-13	52	8
Adherens junction	3.09E-09	44	5	Proteoglycans in cancer	5.86E-13	107	8
Prion diseases	3.09E-09	14	5	TGF- $\beta$ signaling pathway	3.29E-09	49	8
Viral carcinogenesis	1.64E-08	91	5	Viral carcinogenesis	5.77E-09	99	8
Hippo-signaling pathway	2.37E-08	68	5	Cell cycle	2.79E-08	74	8
TGF- $\beta$ signaling pathway	9.56E-08	41	5	Hippo signaling pathway	1.24E-07	74	8
TARGETSCAN				TARGETSCAN			
Fatty acid biosynthesis	7.90E-38	2	2	Fatty acid biosynthesis	2.92E-53	3	1
Fatty acid metabolism	8.15E-15	3	2	Fatty acid metabolism	1.03E-21	4	1
Metabolism of xenobiotics by cytochrome P450	7.48E-06	2	2	Signaling pathways regulating pluri-potency of stem cells	2.58E-09	17	7
Signaling pathways regulating pluri-potency of stem cells	6.26E-05	11	3	Metabolism of xenobiotics by cytochrome P450	8.99E-07	3	3
TGF- $\beta$ signaling pathway	0.0387	5	3	N-Glycan biosynthesis	0.00466	5	3
Micro-CT-DS				Micro-CT-DS			
Fatty acid biosynthesis	7.90E-38	5	2	Fatty acid biosynthesis	7.39E-26	6	9
Fatty acid metabolism	8.15E-15	11	2	ECM-receptor interaction	3.21E-07	17	9
Signaling pathways regulating pluri-potency of stem cells	3.74E-12	47	3	Signaling pathways regulating pluri-potency of stem cells	1.01E-06	43	9
Hippo signaling pathway	2.06E-06	29	2	Mucin type O-Glycan biosynthesis	5.38E-06	9	9
Proteoglycans in cancer	2.70E-06	59	4	Proteoglycans in cancer	2.34E-05	53	9
				p53 signaling pathway	3.13E-05	27	9

<https://doi.org/10.1371/journal.pone.0230092.t006>

the top 16 miRNA whose expression contributed the most to the first and second Principle Components (PC1 and PC2). These components capture factors responsible for the most and second most variation in the data set, respectively. Samples with the most similar miRNA expression profile cluster together and clusters may vary over PC1/PC2 or both (S5 Fig). Twelve miRNA identified in the fold-change analysis of highly inflamed or cancer-infiltrated LVs, were among the top 20 miRNA that contributed to PC1, with 5 of those showing significant differential expression. Furthermore, 8 miRNAs of the top 20 miRNA that contributed to PC2 were all identified as significantly downregulated >1.8 fold in highly inflamed LVs. The remaining miRNA varied greatly between the patient samples, e.g., miR-20, but were not identified by analysis of fold change between groups. The expression levels of these miRNA were therefore spread equally between the compared groups. Overall, variation over PC2

**Table 7. Classification analysis performance for various supervised classification algorithms for the prediction of patient relapse based on LV miRNA expression.**

Method	Accuracy	McNemar's Test-pval	Cohen's Kappa	No Relapse	Yes Relapse
Logistic Regression	70%	0.999	0.375	67%	75%
K-Nearest Neighbours	80%	0.289	0.583	100%	50%
Support Vector Machines	80%	0.289	0.583	100%	50%
Random Forests Classifier	50%	0.375	-0.042	67%	25%
Gaussian Naive Bayes	60%	0.031	0.167	100%	0%

This illustrates the accuracy of the method (percentage of correct predictions), the per-group accuracy (No Relapse, Yes Relapse), Cohen's Kappa of inner agreement between predicted and actual outcome, and McNemar's test of significance of equality of predicted probability (inner accuracy) between groups for each outcome.

<https://doi.org/10.1371/journal.pone.0230092.t007>

differentiates between highly-inflamed and non-inflamed LVs, supporting the suggestion that miRNA expression could distinguish LV states (S5 Fig).

### Application of machine-learning algorithms to predict LV state or clinical outcome based on miRNA expression

Patterns of miRNA expression showed some potential in predicting clinical outcomes by applying classification algorithms. When predicting patient relapse (Table 7), all of the classification methods presented with quite high accuracy values and McNemar's probabilities of  $p < 0.05$ , meaning that no significant difference was found between the predicted grouping, based on miRNA expression, and the grouping based on the known clinical data. Of the methods applied, use of k-Nearest Neighbours and logistic regression produced the highest classification accuracy with similar prediction accuracy achieved between methods. Classification of cancer-cell infiltrated LVs based on miRNA expression (Table 8) showed a similar prediction accuracy compared to classification of relapse LVs, but the Random Forest classifier achieved the best accuracy. Classification of inflamed and  $\leq$  Stage IV samples did not show a high accuracy (S7 Table). As a further evaluation, we examined the effect of keeping as predictors only those miRNAs that have significant associations with the outcome variables. Analysis was performed on classifiers build using only significantly differentially expressed miRNAs ( $p < 0.05$ ). In the cancer-infiltrated LVs, the differentially expressed miRNAs enhanced the accuracy of the predictive algorithm to 80–100% (S8 Table). Prediction of relapse based on miR-23b-3p and miR-186-5p expression, improved the accuracy of classification with all methods by 10%, except when using the Support Vector Machine, where no improvement was observed (see S8 Table & S1 File). The addition of miR-let-7b-5p and let-7c-5p improved the accuracy of the Support Vector Machine from 80% to 90% but decreased the accuracy of Logistic Regression from 80% to 70%. However, the use of miR-23b and miR-186-5p only showed a bias towards classifying the samples as non-relapsed when using Logistic Regression, which decreased when using all 4 miRNA. These results suggest that the miRNAs with

**Table 8. Classification performance of various supervised classification algorithms for the prediction of cancer infiltration based on LV miRNA expression.** Details are similar to Table 7.

Method	Accuracy	McNemar's Test-pval	Cohen's Kappa	No Cancer	Yes Cancer
Logistic Regression	70%	0.44	0.38	83%	50%
K-Nearest Neighbours	50%	0.37	-0.04	67%	25%
Support Vector Machines	70%	0.13	0.37	100%	25%
Random Forests Classifier	100%	1.00	1.00	100%	100%
Gaussian Naive Bayes	50%	0.37	-0.04	67%	25%

<https://doi.org/10.1371/journal.pone.0230092.t008>

significant associations to the outcome variables have a capacity to be used as predictors for predicting the outcomes of interest in new patients.

## Discussion

To our knowledge, this is the first analysis of inflammatory and miRNA alterations in tumour draining LVs in ovarian cancer. In this feasibility study, we aimed to provide insights into LV features that might be associated with patient relapse. Our results may contribute to a better prediction of patient relapse, and could guide future experimental work seeking to improve patient outcome via therapeutic targeting of miRNA.

Macroscopically normal LVs, remote from the tumour site that exhibited high or medium inflammation correlated with cancer relapse. Despite cancer-cell infiltration in 66% of these vessels, a moderate but non-significant association was identified between inflamed and cancer-infiltrated LVs ( $p = 0.07$ ). The staging of LNs is routinely used to quantify cancer progression but the status of the connecting LVs has not previously been investigated. While case numbers are small, the presence of high inflammation in the LVs showed the strongest significant correlation with cancer relapse ( $p = 0.03$   $\kappa = 0.783$ ). The Kaplan Meier estimates of non-relapse also showed that relapse became less likely without the presence of LV inflammation or cancer-cell infiltration, and age did not increase likelihood of relapse (S2 and S3 Figs). Whether inflammation is a consequence of factors that contribute to relapse, or the inflammation-induced changes directly affect relapse, is an area for future work.

Analysis of the effect of cancer cell infiltration of the LVs, without considering LV inflammatory state, identified a trend towards a non-significant association with relapse ( $p = 0.07$ ,  $\kappa = 0.783$ ). This suggests that cancer-infiltration of LVs alone may not necessarily predict relapse, but rather accompanying changes in vessel inflammation may increase the likelihood of relapse. Furthermore, cancer-cell infiltration did not show a significant association with high inflammation. The lack of a significant correlation in both cases may also be simply due to the possible scenario that cancer cells are just transiting through these vessels, so detecting their presence becomes a matter of timing. Overall, this study suggests that nearby LVs appear to play an important role in the immune response to cancer and the association between inflammatory lymphatic changes and relapse deserves further exploration while potentially representing a therapeutic target.

The use of miRNA expression classification algorithms also showed potential to predict relapse, with relatively high accuracy for these 10 patients when applying a k-Nearest Neighbours algorithm or a Support Vector Machine model (80%), rising to 90% when using significantly differentially expressed miRNA only (Tables 7 and S8). Further studies spanning a larger number of patients should therefore be performed. Clinically, the prediction of a patient's outcome based on miRNA expression of tissue collected during surgery could be of considerable value. Despite the presence of inflammation showing a moderate agreement with relapse and high inflammation displaying a significant correlation with relapse, a classifier based on miRNA expression in high or medium inflamed LVs did not show a high accuracy (Tables 2, 3, S7 and S8). Furthermore, due to the limited number of highly inflamed LVs, it was not possible to build a reliable classifier based on miRNA expression in LVs with high inflammation versus miRNA expression in LVs with low or medium inflammation. Indeed, all the classifiers are limited by the number of samples required to train the predictive algorithms. Therefore, whilst providing insight, these observations require increased sample input to maintain confidence in miRNA classification.

Analysis of miRNA expression of highly inflamed LVs compared to LVs with no or low inflammation, showed down-regulation of 6 members of the let-7 family, 3 of which remained

significant with a Bonferroni correction ( $p < 0.0017$ ). A similar trend was observed when comparing miRNA expression of LVs presenting with high or medium inflammation to those with low inflammation. In this case 6 members of the let-7 family showed down-regulation  $> 1.8$  fold but only two members showed significant down-regulation ( $p < 0.05$ ), which may be reflective of less difference in mean LV inflammatory state between the two groups compared. The change in let-7 miRNA expression was large enough that without designating groups, the overall variability in sample miRNA expression due to let-7 expression could be detected using PCA (S5 Fig). In ovarian tumour tissue, let-7 expression is down-regulated and associated with poor prognosis and chemo-resistance [17,30,31]. Let-7 family members target oncogenes HMAG2 and RAS, and loss of let-7 is also associated with the development of aggressive cancers [32]. Chemo-sensitivity of tumours may also be affected by let-7 expression. Manipulation of let-7e in EOC cells *in-vitro* and *in-vivo* confirmed that expression is reduced in cisplatin-resistant cell lines and application of let-7e mimics alongside cisplatin, reduced tumour growth in mice more than with cisplatin alone [33]. Furthermore, chimeric-mediated delivery of let-7i miRNA to EOC cells *in-vitro* reversed paclitaxel-induced chemo-resistance [34]. Expression of let-7 is also associated with control of the Cdk-dependent cell cycle network, that drives the cell transformation network, allowing cells to undergo an epigenetic switch between non-transformed and a malignant transformed state [35].

The implications of let-7 down-regulation in LVs include changes in immune response and LV permeability. Members of the let-7 family can target inflammatory cytokines, such as IL-6 by let-7a and IL-13 by let-7f, shown to contribute to cancer-cell apoptosis and anti-inflammatory action respectively [36,37]. In addition to affecting immune cells in transit, drainage of cytokines to LNs could impact immune response at the LN, potentially contributing to the loss of immuno-suppression observed in draining LNs [38]. Cytokines may also affect LV transport, as IL-6 can increase LV permeability while intradermal administration of cytokines IL-1 $\beta$ , TNF- $\alpha$ , and IL-6 have been shown to decrease lymphatic contraction frequency [39,40]. Down-regulation of let-7 in vascular endothelial cells is associated with increased TGF- $\beta$  signalling leading to promotion of epithelial-to-mesenchymal transition and thus increased vessel permeability, but the effects in LVs are currently unknown [41]. The observed up-regulation of several miRNA (miR-381-3p, miR-93-5p, miR-16-5p and miR-497-5p) in cancer-infiltrated LVs may inhibit Vascular Endothelial Growth Factor (VEGF) expression or VEGF receptors, both directly and indirectly via Bcl-2 inhibition [42–45]. The inhibition of VEGF secretion in tumours has been a target of several drug trials but manipulation of VEGF secretion in connecting LVs may present as a future therapeutic area [46]. Expression of miR-144 has been shown to target RUNX-1 in EOC lines and SRF in HUVECs, both contributing to anti-proliferative action. A more extensive list of potential targets is provided in Table 9. A logical progression of this study would be to confirm targets in LECs.

Further studies of the relationship between inflammatory markers in LVs and differential miRNA expression would increase the potential for diagnostic capabilities. Jones et al. and Yee et al., analyzed LEC responses to inflammation and identified a total of 16 differentially expressed miRNA, one of which (miR-17-5p) overlapped with the panel of miRNAs screened in our study [18,19]. Chakraborty et al., identified differentially expressed miRNA associated with autoimmunity and inflammation in rat LECs, with different sets of miRNAs identified at 2 hours, 48 hours and 96 hours after induction of inflammation [13]. Our results showed no overlap with the miRNAs regulated at the 2-hour time-point but did show similar upregulation of miR-19a detected at 48 hours and induction of miR-497, miR-19b and miR-19a observed at 96 hours [13]. Additionally, there was no evidence of dysregulation of the let-7 family in the rat LECs. Taken together, chronic inflammation of LVs in EOC patients may impact miRNA

**Table 9. Confirmed targets of miRNA in primarily endothelial and cancer cell lines identified as significantly differentially regulated between groups.**

miRNA	Target	Cell type	Pathway/Function	Ref.
let7 family	RAS	EOC lines	tumour/Ras/MAPK-suppressor	[47]
	HMAG2	EOC lines	anti-apoptotic, tumour-suppressor	[48]
	indirect	HUAECs	inhibits TGF $\beta$ pathway, pro-EMT	[41]
let7a-5p	IL6	Epithelial cells	pro-cancer-cell survival	[36]
	TGFBR3	HUVECs	anti-angiogenic, anti-tube formation	[49]
	LOX-1	HUVECs	anti-apoptotic, pro NO synthesis	[50]
let7b-5p	LOX-1	HUVECs	anti-apoptotic, pro NO synthesis	[50]
let7c-5p	Bcl-xl	HUVECs	pro-apoptotic, via ox-LDL induced apoptosis	[51]
let7d-5p	IFI44L	HUVECs	anti-proliferation/migration	[52]
let7e-5p	Il $\beta$	HUVECs	pro-Nf $\kappa$ $\beta$ pathway	[53]
let7f-5p	IL10	CD4 <sup>+</sup> T cells	pro-inflammatory	[54]
	IL3	Lymphocytes	anti-inflammatory	[37]
let7g-5p	LOX-1	VSCMs	anti-apoptotic	[55]
	TGFBR3/ SMAD2 /THBS	HUVECs	pro-angiogenic, targets TF $\beta$ pathway	[56]
	IL10	TH1/TH17 T cells	pro-inflammatory	[57, 58]
miR-93-5p	EPLIN	HUVECS	pro-proliferative/migration/angiogenesis	[59]
	PTEN	OC lines	anti-apoptotic miR93-5p/PTEN/pAkt	[60]
	RhoC	EOC lines	pro-apoptotic, anti-migration	[61]
	IL8	Neuroblastoma	anti-angiogenic	[43]
	VEGF	Neuroblastoma	anti-angiogenic	[43]
miR-144-3p	Meis1	Embryotic (Zebrafish)	decreases runx-1,c-myc, haematoepoeieisis	[62]
	SRF	HUVECs	anti-proliferative, pro-apoptotic	[63]
	RUNX-1	EOC lines	anti-proliferation, anti-migration	[64]
miR-23a-3p	ZO-2 & JAM-C	HUVECs	inhibit permeability	[65]
	RUNX2	HUVECs	anti-angiogenic, suppresses VEGF-A	[66]
miR-23b-3p	JAM-C & ZO-2	HUVECs	pro-angiogenic, increase permeability	[65]
	TAB2,TAB3, IKKa	Lymphocytes	suppresses IL-17-associated inflammation	[67]

EOC = Epithelial ovarian cancer.

EMT = Epithelial-to-Mesenchymal Transition.

HUVEC = Human umbilical vascular endothelial cells.

HUAEC = Human umbilical arterial endothelial cells.

<https://doi.org/10.1371/journal.pone.0230092.t009>

expression differently, aligning more closely with the later time-points post-inflammatory induction in the controlled rat experiments.

The pathway analysis of the dysregulated miRNA identified involvement in transforming-growth factor TGF- $\beta$ 2 signalling, as well as glycoproteins in cancer and molecules that contribute to the glycocalyx of the LV lumen (Table 6). LECs possess a glycocalyx composed of glycoprotein side chains, a backbone that includes adhesion molecules, and a proteoglycan core. Therefore, changes to glycoproteins or adherens junctions may affect integrity of the LV wall [68]. Furthermore, a study by Zolla et al. showed aged collecting LVs in rats presented with a thinner endothelial cell glycocalyx and a loss of gap junction proteins [69]. Functionally this resulted in hyper-permeability of the LVs that allowed pathogens to escape into surrounding tissue. This may suggest that the miRNA changes that accompany cancer cell infiltration and inflammation may also alter LV permeability and barrier function. This in turn could aid cancer cell infiltration but may also impact similar movements of immune cells such as macrophages and dendritic cells [70]. Further studies to assess the impact of inflammation-induced

miRNA expression changes on LV integrity may identify new avenues to prevent transmigration of cancer cells across LV walls.

The response to cancer may also be mediated by inflammatory cells normally present in the LV. Analysis of rat mesenteric, pre-nodal and post-nodal LVs has shown the presence of innate inflammatory immune cells accumulating on the walls of the LVs including neutrophils, monocytes and macrophages [70]. Microarray analysis of mesenteric collecting vessels has also shown significant accumulation of MHCII+ antigen-presenting cells [71]. Furthermore, both antigen-presenting cells and T cells are transported in LVs, with proportions depending on the status of the upstream tissues [72]. We have not assessed the status of all of the tissues drained by these LVs, but in any case we would expect some immune cells to be captured in our images. However, the overall proportion of T cells to LV wall structural cells should be low enough not to impact overall miRNA expression.

The expression of the enzyme myeloperoxidase (MPO) was selected as an inflammatory marker due to evidence supporting MPO as a reliable inflammatory marker in a range of pathogenesis including cancer, rheumatoid arthritis and cardiovascular disease in addition to tissue injury [73]. The expression of MPO has also been associated with ovarian epithelial carcinoma cells in early stage carcinomas [74]. Presence of MPO is also specifically associated with vascular vessel inflammation [75,76]. Furthermore, MPO has been used as a reliable indicator of lymphatic vessel inflammatory status to quantify LPS-induced lymphatic vessel inflammation in rats in conjunction with Masson Trichome staining to indicate fibrotic vessel areas [13]. Other indicators of inflammatory state could be used, perhaps benefitting the prognostic value for relapse.

A significant limitation of our feasibility study is the small sample size. Although we have successfully identified associations with high potential for outcomes prediction, further samples could both strengthen the trends observed and uncover more obscure alterations associated with inflammation and/or relapse. Additionally, it is possible that increasing sample size could result in the identification of inflamed but non-cancer infiltrated LVs. However, there is no guarantee that increasing sample size would lead to the emergence of this group. The sample size also contributed to the decision to perform real time PCR with a relatively small number of pre-selected targets. A broader microarray study would require many more samples to avoid false positives. We screened for miRNA with known involvement in inflammatory and autoimmunity due to the previous characterization of inflammatory vessel state and pathophysiological changes associated with inflammation and lymphatic function in rat lymphatic vessels [13].

A further limitation to this study is the lack of samples from healthy controls. Harvesting equivalent lymphatic tissues from healthy patients would not be ethical. However, this means that the changes in LV status noted here are more directly relevant to identification of factors that aid prognosis than identifying systemic EOC changes compared to healthy subjects. Epithelial ovarian cancer surgical techniques and types of cytotoxic treatments do not differ, as of yet, between the various histological subtypes. We therefore included all available epithelial subtypes, even the clear cell case, to have a broader representation of the clinical reality. Although our results support a link between systemic inflammation and cancer cell dissemination, a larger study is warranted to validate our findings and to allow further analysis to better identify miRNA patterns using predictive algorithms with greater confidence.

## Conclusions

In conclusion, we have demonstrated that LVs appear to show quantifiable inflammatory and infiltrative alterations in patients with advanced EOC and that a high inflammatory LV state

significantly correlates with higher risk of post-surgical relapse. Macroscopically normal lymphatic LVs show accompanying alterations in miRNA expression that may impact LV integrity and secretion of VEGF and inflammatory cytokines. Whether LV inflammation is a cause or consequence of cancer-cell infiltration is yet to be determined, but our results suggest systemic inflammation as a new area to target.

## Supporting information

**S1 File. Supplementary information regarding building supervised classification algorithms.** The techniques and assumptions when building classification algorithms and assessing the impact of individual miRNA.

(PDF)

**S1 Fig. Experimental design for LV miRNA analysis from sample collection to analysis.**

Each vessel dissected from one sample is divided into 2 and processed for IHC and miRNA expression analysis.

(JPEG)

**S2 Fig. Kaplan Meier estimates of non-relapse (survival).** A. According to inflammation (MPO) (high vs. medium/low) B. According to inflammation (MPO) (high/medium vs. low). C. According to cancer cell infiltration (WT1 or Pax.8).

(TIF)

**S3 Fig. Kaplan Meier estimates of non-relapse (survival) according to multiple patient age thresholds.** A. Under 55 years B. Under 60 years C. Under 65 years. D Under 70years. E Under 75years.

(TIF)

**S4 Fig. The KDE estimations of the distributions of inner groups for the individual miRNA expressed at statistically significant levels ( $p < 0.05$ ) between LVs with high inflammation and LVs with low inflammation.**

(JPEG)

**S5 Fig.** A. Principle component analysis showed that inflamed and non-inflamed samples show variance across Principle Component (PC) 2. Samples with most similar miRNA expression profile cluster together. Unit variance scaling was applied to rows; SVD with imputation was used to calculate principal components. Prediction ellipses are such that with probability 0.95, a new observation from the same group will fall inside the ellipse.  $N = 10$  data points. Figures produced with ClustVis [26] B. The miRNA expression driving PC1 & 2 contributed to the greatest variation between sample groups with several miRNA identified as differentially regulated when comparing inflamed or cancer-infiltrated LVs (bold =  $> \pm 1.8$ , \* =  $p < 0.05$ ). C. A Scree plot showing the amount of variation described by each PC confirmed that the two primary PCs accounted for much of the variation between all sample.

(PDF)

**S1 Table. Additional clinical data (patient age and surgery type).**

(PDF)

**S2 Table. Differential expression of miRNA between LVs displaying high or low inflammation.** We compared expression in LVs with high versus low inflammation ( $n = 7$ ) Listed are miRNA that showed a fold-regulation change  $\pm 1.8$  with those showing a significant difference between groups highlighted (t-test  $p > 0.05$ ). \* = miRNA that remained below a Bonferroni

correction of  $p < 0.00208$ .  
(PDF)

**S3 Table. Differential expression of miRNA between LVs displaying high or low inflammation.** We compared expression in LVs with high or medium inflammation versus low inflammation ( $n = 10$ ) Listed are miRNA that showed a fold-regulation change  $\pm 1.8$  with those showing a significant difference between groups highlighted (t-test  $p > 0.05$ ). \* = miRNA that remained below a Bonferroni correction of  $p < 0.00161$ .  
(PDF)

**S4 Table. Differential expression of miRNA between cancer-infiltrated LVs and non-cancer-infiltrated LVs.** Listed are miRNA that showed a fold-regulation change  $\pm 1.8$  with those showing a significant difference between groups highlighted (t-test  $p > 0.05$ ). \* = miRNA that remained below a Bonferroni correction of  $p < 0.002$ .  
(PDF)

**S5 Table. Differential expression of miRNA in LVs from patients that relapsed versus LVs from patients that didn't relapse within 13.2 $\pm$ 6 months.** Listed are miRNA that showed a fold-regulation change  $\pm 1.8$  with those showing a significant difference between groups highlighted (t-test  $p > 0.05$ ). Bonferroni correction of  $p < 0.002$ .  
(PDF)

**S6 Table. Table of classification analysis for various supervised classification algorithms to predict LV inflammation (low or medium/high) or patient stage from LV miRNA expression.** Depicted is the accuracy of the algorithm to predict LV inflammation or patient relapse (percentage of correct predictions), the per-group accuracy (No Inflamm., Yes Inflamm. / Stage  $< IV$ , Stage  $> = IV$ ), Cohen's Kappa and thus the agreement between predicted and actual states, and McNemar's test significance of equality of predicted probability (inner accuracy) between groups for each outcome.  
(PDF)

**S7 Table. Classifier predictions of the examined states (LV inflammation, LV cancer-cell infiltration, patient relapse or patient stage) based on the expression of significantly dysregulated miRNA.** Accuracy, Cohen's Kappa, Mc Nemar p-value of equality for inner grouped probabilities and classification are reported for the predicted classes. The expression of the most significantly differentially expressed miRNA were added one by one, or in pairs if significance was equal, into the parameter set used to build the classifiers. When only significantly differentially expressed miRNA identified in inflamed LVs (high and medium inflammation versus low) were used to build the classifier, the accuracy of subsequent predictions increased by 20–40% compared to classifiers based on all available miRNA expression (S6 Table). Similar improvements were found in the accuracy of classifiers predicting relapse and LV cancer-infiltration (Tables 7 and 8).  
(PDF)

**S8 Table. Pathway-analysis performed with the 3 significantly up-regulated and single significantly down-regulated miRNA identified in the relapse versus non-relapse groupings.**  
(PDF)

## Acknowledgments

The authors gratefully acknowledge the provision of tissue samples by the Imperial College Healthcare NHS Trust Tissue Bank. Other investigators may have received samples from these

same tissues. The research was supported by the Experimental Cancer Medicine Centre (ECMC, Hammersmith Campus) and National Institute for Health Research (NIHR) Biomedical Research Centre based at Imperial College Healthcare NHS Trust and Imperial College London. We also thank Dr Ilias Kalamaras for his assistance. The views expressed are those of the author(s) and not necessarily those of the NHS, the NIHR or the Department of Health.

## Author Contributions

**Conceptualization:** Sanjukta Chakraborty, David C. Zawieja, Mariappan Muthuchamy, Christina Fotopoulou, James E. Moore Jr.

**Data curation:** Sarah C. Johnson.

**Formal analysis:** Anastasios Drosou, Dimitrios Tzovaras.

**Funding acquisition:** David C. Zawieja, Christina Fotopoulou, James E. Moore Jr.

**Investigation:** Sarah C. Johnson, Christina Fotopoulou, James E. Moore Jr.

**Methodology:** Sarah C. Johnson, Sanjukta Chakraborty, Paula Cunnea, Katherine Nixon, Christina Fotopoulou.

**Project administration:** Paula Cunnea, Katherine Nixon, James E. Moore Jr.

**Resources:** Paula Cunnea, Katherine Nixon, David C. Zawieja, Mariappan Muthuchamy, Christina Fotopoulou, James E. Moore Jr.

**Supervision:** Sanjukta Chakraborty, Christina Fotopoulou, James E. Moore Jr.

**Visualization:** Sarah C. Johnson.

**Writing – original draft:** Sarah C. Johnson.

**Writing – review & editing:** Sarah C. Johnson, Paula Cunnea, Mariappan Muthuchamy, Christina Fotopoulou, James E. Moore Jr.

## References

1. UK CR. Cancer Research UK. 2018. Available from: <https://www.cancerresearchuk.org/health-professional/cancer-statistics/statistics-by-cancer-type/ovarian-cancer>.
2. Bachmann C, Bachmann R, Kraemer B, Brucker SY, Staebler A, Fend F, et al. Prevalence and distribution pattern of nodal metastases in advanced ovarian cancer. *Molecular and Clinical Oncology*. 2016; 5(4):483–487. <https://doi.org/10.3892/mco.2016.982> PMID: 27703680
3. Bachmann C, Bachmann R, Fend F, Wallwiener D. Incidence and Impact of Lymph Node Metastases in Advanced Ovarian Cancer: Implications for Surgical Treatment. *Journal of Cancer*. 2016; 7(15):2241–2246. <https://doi.org/10.7150/jca.15644> PMID: 27994660
4. Wimberger P, Lehmann N, Kimmig R, Burges A, Meier W, Bois AD. Prognostic factors for complete debulking in advanced ovarian cancer and its impact on survival. An exploratory analysis of a prospectively randomized phase III study of the Arbeitsgemeinschaft Gynäkologische Onkologie Ovarian Cancer Study Group (AGO-OVAR). *Gynecologic Oncology*. 2007; 106(1):69–74. <https://doi.org/10.1016/j.ygyno.2007.02.026> PMID: 17397910
5. Harter P, Sehouli J, Lorusso D, Reuss A, Vergote I, Marth C, et al. A Randomized Trial of Lymphadenectomy in Patients with Advanced Ovarian Neoplasms. *N Engl J Med*. 2019; 380(9):822–832 <https://doi.org/10.1056/NEJMoa1808424> PMID: 30811909
6. Padera TP, Kadambi A, Tomaso E, Carreira CM, Brown EB, Boucher Y, et al. Lymphatic Metastasis in the Absence of Functional Intratumor Lymphatics. *Science*. 2002; 296(5574):1883–1886. <https://doi.org/10.1126/science.1071420> PMID: 11976409
7. Leu AJ, Berk DA, Lymboussaki A, Alitalo K, Jain RK. Absence of Functional Lymphatics within a Murine Sarcoma: A Molecular and Functional Evaluation. *Cancer Research*. 2000; 60(16):4324–4327. PMID: 10969769

8. Jones D, Pereira ER, Padera TP. Growth and Immune Evasion of Lymph Node Metastasis. *Frontiers in oncology*. 2018; 8:36;36–36.
9. Stachura J, Wachowska M, Kilarski WW, Güc E, Golab J, Muchowicz A. The dual role of tumor lymphatic vessels in dissemination of metastases and immune response development. *Oncoimmunology*. 2016; 5(7): e1182278. <https://doi.org/10.1080/2162402X.2016.1182278> PMID: 27622039
10. Dieterich LC, Ikenberg K, Cetintas T, Kapaklikaya K, Huttmacher C, Detmar M. Tumor- Associated Lymphatic Vessels Upregulate PDL1 to Inhibit T-Cell Activation. *Frontiers in immunology*. 2017; 8:66. <https://doi.org/10.3389/fimmu.2017.00066> PMID: 28217128
11. Lund A, Duraes F, Hirosue S, Raghavan V, Nembrini C, Thomas S, et al. VEGF-C Promotes Immune Tolerance in B16 Melanomas and Cross-Presentation of Tumor Antigen by Lymph Node Lymphatics. *Cell Reports*. 2012; 1(3):191–199. <https://doi.org/10.1016/j.celrep.2012.01.005> PMID: 22832193
12. Dubrot J, Duraes FV, Potin L, Capotosti F, Brighouse D, Suter T, et al. Lymph node stromal cells acquire peptide–MHCII complexes from dendritic cells and induce antigen-specific CD4+ T cell tolerance. *Journal of Experimental Medicine*. 2014; 211(6):1153–1166. <https://doi.org/10.1084/jem.20132000> PMID: 24842370
13. Chakraborty S, Zawieja DC, Davis MJ, Muthuchamy M. MicroRNA signature of inflamed lymphatic endothelium and role of miR-9 in lymphangiogenesis and inflammation. *American Journal of Physiology—Cell Physiology*. 2015; 309(10):C680–C692. <https://doi.org/10.1152/ajpcell.00122.2015> PMID: 26354749
14. Liao S, Cheng G, Conner DA, Huang Y, Kucherlapati RS, Munn LL, et al. Impaired lymphatic contraction associated with immunosuppression. *Proceedings of the National Academy of Sciences of the United States of America*. 2011; 108(46):18784–18789. <https://doi.org/10.1073/pnas.1116152108> PMID: 22065738
15. Calin GA, Croce CM. MicroRNA signatures in human cancers. *Nature Reviews Cancer*. 2006; 6: 857–866. <https://doi.org/10.1038/nrc1997> PMID: 17060945
16. Deb B, Uddin A, Chakraborty S. miRNAs and ovarian cancer: An overview. *Journal of Cellular Physiology*. 2018; 233(5):3846–3854. <https://doi.org/10.1002/jcp.26095> PMID: 28703277
17. Dahiya N, Sherman-Baust CA, Wang TL, Davidson B, Shih I, Zhang Y, et al. MicroRNA Expression and Identification of Putative miRNA Targets in Ovarian Cancer. *PLOS ONE*. 2008; 3(6):1–11.
18. Jones D, Li Y, He Y, Xu Z, Chen H, Min W. Mirtron MicroRNA-1236 Inhibits VEGFR- 3 Signaling during Inflammatory Lymphangiogenesis. *Arteriosclerosis, Thrombosis, and Vascular Biology*. 2012; 32(3):633–642. <https://doi.org/10.1161/ATVBAHA.111.243576> PMID: 22223733
19. Yee D, Shah KM, Coles MC, Sharp TV, Lagos D. MicroRNA-155 induction via TNF- and IFN-suppresses expression of programmed death ligand-1 (PD-L1) in human primary cells. *The Journal of Biological Chemistry*. 2017; 292(50):20683–20693. <https://doi.org/10.1074/jbc.M117.809053> PMID: 29066622
20. Sasahira T, Kurihara M, Bhawal UK, Ueda N, Shimomoto T, Yamamoto K, et al. Downregulation of miR-126 induces angiogenesis and lymphangiogenesis by activation of VEGF-A in oral cancer. *British Journal of Cancer*. 2012; 107:700–706. <https://doi.org/10.1038/bjc.2012.330> PMID: 22836510
21. Hu J, Cheng Y, Li Y, Jin Z, Pan Y, Liu G, et al. microRNA-128 plays a critical role in human non-small cell lung cancer tumorigenesis, angiogenesis and lymphangiogenesis by directly targeting vascular endothelial growth factor-C. *European Journal of Cancer*. 2014; 50(13):2336–2350. <https://doi.org/10.1016/j.ejca.2014.06.005> PMID: 25001183
22. Yang B, Jing C, Wang J, Guo X, Chen Y, Xu R, et al. Identification of microRNAs associated with lymphangiogenesis in human gastric cancer. 2013;16.
23. Xu J, Zhang C, He Y, Wu H, Wang Z, Song W, et al. Lymphatic endothelial cell-secreted CXCL1 stimulates lymphangiogenesis and metastasis of gastric cancer. *International Journal of Cancer*. 2012; 130(4):787–797. <https://doi.org/10.1002/ijc.26035> PMID: 21387301
24. Schindelin J, Arganda-Carreras I, Frise E, Kaynig V, Longair M, Pietzsch T, et al. Fiji: an open-source platform for biological-image analysis. *Nature Methods*. 2012; 9:676–682. <https://doi.org/10.1038/nmeth.2019> PMID: 22743772
25. Vierra A, Garret J. Understanding Interobserver Agreement: The Kappa Statistic. *Research Series*. 2005; 37(5).
26. Metsalu T, Vilo J. ClustVis: a web tool for visualizing clustering of multivariate data using Principal Component Analysis and heatmap. *Nucleic Acids Research*. 2015; 43(W1):W566–W570. <https://doi.org/10.1093/nar/gkv468> PMID: 25969447
27. Vlachos I.S, Hatzigeorgiou AG. DIANA-miRPath v3. 0: deciphering microRNA function with experimental support. *Nucleic acids research*. 2015; 43:W460–W466. <https://doi.org/10.1093/nar/gkv403> PMID: 25977294

28. Edgar R, Domrachev M, Lash AE. Gene Expression Omnibus: NCBI gene expression and hybridization array data repository. *Nucleic acids research*. 2002 01; 30(1):207–210. <https://doi.org/10.1093/nar/30.1.207> PMID: 11752295
29. Bhattacharya R, Nicoloso M, Arvizo R, Wang E, Cortez A, Rossi S, et al. MiR-15a and MiR-16 Control Bmi-1 Expression in Ovarian Cancer. *Cancer Research*. 2009; 69(23):9090–9095. <https://doi.org/10.1158/0008-5472.CAN-09-2552> PMID: 19903841
30. Petrillo M, Zannoni GF, Beltrame L, Martinelli E, DiFeo A, Paracchini L, et al. Identification of high-grade serous ovarian cancer miRNA species associated with survival and drug response in patients receiving neoadjuvant chemotherapy: a retrospective longitudinal analysis using matched tumor biopsies. *Annals of Oncology*. 2016; 27(4):625–634. <https://doi.org/10.1093/annonc/mdw007> PMID: 26782955
31. Sorrentino A, Liu CG, Addario A, Peschle C, Scambia G, Ferlini C. Role of microRNAs in drug-resistant ovarian cancer cells. *Gynecologic Oncology*. 2008; 111(3):478–486. <https://doi.org/10.1016/j.ygyno.2008.08.017> PMID: 18823650
32. Boyerinas B, Park SM, Hau A, Murmann AE, Peter ME. The role of let-7 in cell differentiation and cancer. *MicroRNA*. 2012; 1(1):34–39. <https://doi.org/10.2174/2211536611201010034>
33. Cai J, Yang C, Yang Q, Ding H, Jia J, Guo J, et al. Deregulation of let-7e in epithelial ovarian cancer promotes the development of resistance to cisplatin. *Oncogenesis*. 2013; 2:e75 <https://doi.org/10.1038/oncsis.2013.39> PMID: 24100610
34. Liu N, Zhou C, Zhao J, Chen Y. Reversal of Paclitaxel Resistance in Epithelial Ovarian Carcinoma Cells by a MUC1 Aptamer-let-7i Chimera. *Cancer Investigation*. 2012; 30(8):577–582. <https://doi.org/10.3109/07357907.2012.707265> PMID: 22812695
35. Gérard C, Lemaigre F, Gonze D. Modeling the Dynamics of Let-7-Coupled Gene Regulatory Networks Linking Cell Proliferation to Malignant Transformation. *Frontiers in Physiology*. 2019; 10:848. <https://doi.org/10.3389/fphys.2019.00848> PMID: 31354514
36. Meng F, Henson R, Wehbe-Janek H, Smith H, Ueno Y, Patel T. The MicroRNA let-7a Modulates Interleukin-6-dependent STAT-3 Survival Signaling in Malignant Human Cholangiocytes. *Journal of Biological Chemistry*. 2007; 282(11):8256–8264. <https://doi.org/10.1074/jbc.M607712200> PMID: 17220301
37. Kumar M, Ahmad T, Sharma A, Mabalirajan U, Kulshreshtha A, Agrawal A, et al. Let-7 microRNA-mediated regulation of IL-13 and allergic airway inflammation. *Journal of Allergy and Clinical Immunology*. 2011; 128(5):1077–1085.e10. <https://doi.org/10.1016/j.jaci.2011.04.034> PMID: 21616524
38. Choudhury S, Li Y. miR-21 and let-7 in the Ras and NF- $\kappa$ B Pathways. *MicroRNA*. 2012; 1(1):65–69. <https://doi.org/10.2174/2211536611201010065> PMID: 25048092
39. Cromer WE, Zawieja SD, Tharakan B, Childs EW, Newell MK, Zawieja DC. The effects of inflammatory cytokines on lymphatic endothelial barrier function. *Angiogenesis*. 2014; 17(2):395–406. <https://doi.org/10.1007/s10456-013-9393-2> PMID: 24141404
40. Aldrich MB, Sevick-Muraca EM. Cytokines are systemic effectors of lymphatic function in acute inflammation. *Cytokine*. 2013; 64(1):362–369. <https://doi.org/10.1016/j.cyto.2013.05.015> PMID: 23764549
41. Chen PY, Qin L, Barnes C, Charisse K, Yi T, Zhang X, et al. FGF Regulates TGF- $\beta$ 1 Signaling and Endothelial-to-Mesenchymal Transition via Control of let-7 miRNA Expression. *Cell Reports*. 2012; 2(6):1684–1696. <https://doi.org/10.1016/j.celrep.2012.10.021> PMID: 23200853
42. Sun CY, She XM, Qin Y, Chu ZB, Chen L, Ai LS, et al. miR-15a and miR-16 affect the angiogenesis of multiple myeloma by targeting VEGF. *Carcinogenesis*. 2012;34.
43. Metsalu T, Vilo J. MicroRNA miR-93-5p regulates expression of IL-8 and VEGF in neuroblastoma SK-N-AS cells. *Oncol Rep*. 2016; 35(5):2866–72. <https://doi.org/10.3892/or.2016.4676> PMID: 26986724
44. Tzeng HE, Chang AC, Tsai CH, Wang SW, Tang CH. Basic fibroblast growth factor promotes VEGF-C-dependent lymphangiogenesis via inhibition of miR-381 in human chondrosarcoma cells. *Oncotarget*. 2016; 7(25):38566–38578. <https://doi.org/10.18632/oncotarget.9570> PMID: 27229532
45. Yang G, Xiong G, Cao Z, Zheng S, You L, Zhang T, et al. miR-497 expression, function and clinical application in cancer. *Oncotarget*. 2016; 7(34):55900–55911. <https://doi.org/10.18632/oncotarget.10152> PMID: 27344185
46. Giacca M, Zacchigna S. VEGF gene therapy: therapeutic angiogenesis in the clinic and beyond. *Gene Therapy*. 2012; 19:622–629. <https://doi.org/10.1038/gt.2012.17> PMID: 22378343
47. Park SM, Shell S, Radjabi AR, Schickel R, Feig C, Boyerinas B, et al. Let-7 Prevents Early Cancer Progression by Suppressing Expression of the Embryonic Gene HMGA2. *Cell Cycle*. 2007; 6(21):2585–2590. <https://doi.org/10.4161/cc.6.21.4845> PMID: 17957144
48. Johnson SM, Grosshans H, Shingara J, Byrom M, Jarvis R, Cheng A, et al. RAS Is Regulated by the let-7 MicroRNA Family. *Cell*. 2005; 120(5):635–647. <https://doi.org/10.1016/j.cell.2005.01.014> PMID: 15766527

49. Wang S, Zhou H, Wu D, Ni H, Chen Z, Chen C, et al. MicroRNA let-7a regulates angiogenesis by targeting TGFBR3 mRNA. *Journal of Cellular and Molecular Medicine*. 2019; 23(1):556–567 <https://doi.org/10.1111/jcmm.13960> PMID: 30467960
50. Mh Bao, Yw Zhang, Xy Lou, Cheng Y Zhou Hh. Protective Effects of Let-7a and Let-7b on Oxidized Low-Density Lipoprotein Induced Endothelial Cell Injuries. *PLOS ONE*. 2014 09; 9(9):1–10.
51. Bing Q, Xiao B, Liang D, Li Y, Jiang T, Yang H. MicroRNA Let-7c Inhibits Bcl- XI Expression and Regulates Ox-LDL-Induced Endothelial Apoptosis. *BMB Reports*. 2012; 45(8):464–69. <https://doi.org/10.5483/BMBRep.2012.45.8.033> PMID: 22917031
52. Ji X, Hua H, Shen Y, Bu S, Yi S. Let-7d modulates the proliferation, migration, tubulogenesis of endothelial cells. *Molecular and Cellular Biochemistry*. 2019; 462(1):75–83.
53. Lin Z, Ge J, Wang Z, Ren J, Wang X, Xiong H, et al. Let-7e modulates the inflammatory response in vascular endothelial cells through ceRNA crosstalk. *Scientific Reports*. 2017 02; 7:42498 <https://doi.org/10.1038/srep42498> PMID: 28195197
54. Swaminathan S, Suzuki K, Seddiki N, Kaplan W, Cowley MJ, Hood CL, et al. Differential Regulation of the Let-7 Family of MicroRNAs in CD4+ T Cells Alters IL- 10 Expression. *The Journal of Immunology*. 2012; 188(12):6238–6246. <https://doi.org/10.4049/jimmunol.1101196> PMID: 22586040
55. Ding Z, Wang X, Schnackenberg L, Khaidakov M, Liu S, Singla S, et al. Regulation of autophagy and apoptosis in response to ox-LDL in vascular smooth muscle cells, and the modulatory effects of the microRNA hsa-let-7g. *International Journal of Cardiology*. 2013; 168(2):1378–1385. <https://doi.org/10.1016/j.ijcard.2012.12.045> PMID: 23305858
56. Liao YC, Wang YS, Guo YC, Lin WL, Chang MH, Juo SHH. Let-7g Improves Multiple Endothelial Functions Through Targeting Transforming Growth Factor-Beta and SIRT- 1 Signaling. *Journal of the American College of Cardiology*. 2014; 63(16):1685–1694. <https://doi.org/10.1016/j.jacc.2013.09.069> PMID: 24291274
57. Kagawa T, Watanabe M, Inoue N, Otsu H, Saeki M, Katsumata Y, et al. Increases of microRNA let-7e in peripheral blood mononuclear cells in Hashimoto's disease. *Endocrine Journal*. 2016; 63(4):375–380. <https://doi.org/10.1507/endocrj.EJ15-0577> PMID: 26821743
58. Guan H, Fan D, Mrelashvili D, Hao H, Singh N, Singh U, et al. MicroRNA let-7e is associated with the pathogenesis of experimental autoimmune encephalomyelitis. *European journal of immunology*. 2013 01; 43.
59. Liang L, Zhao L, Zan Y, Zhu Q, Ren J, Zhao X. MiR-93-5p enhances growth and angiogenesis capacity of HUVECs by down-regulating EPLIN. *Oncotarget*. 2017 11; 8(63):107033–107043. <https://doi.org/10.18632/oncotarget.22300> PMID: 29291009
60. Fu X, Tian J, Zhang L, Chen Y, Hao Q. Involvement of microRNA-93, a new regulator of PTEN/Akt signaling pathway, in regulation of chemotherapeutic drug cisplatin chemosensitivity in ovarian cancer cells. *FEBS Letters*; 586(9):1279–1286. <https://doi.org/10.1016/j.febslet.2012.03.006> PMID: 22465665
61. Chen X, Chen S, Xiu YL, Sun KX, Zong ZH, Zhao Y. RhoC is a major target of microRNA-93-5P in epithelial ovarian carcinoma tumorigenesis and progression. *Molecular cancer*. 2015 02; 14(1):31; 31–31.
62. Su Z, Si W, Li L, Zhou B, Li X, Xu Y, et al. MiR-144 regulates hematopoiesis and vascular development by targeting meis1 during zebrafish development. *The International Journal of Biochemistry Cell Biology*. 2014; 49:53–63. <https://doi.org/10.1016/j.biocel.2014.01.005> PMID: 24448023
63. Honglei Y, Lihua Z, Junbiao Z, Yan Z. miR-144 regulates the proliferation of human vascular endothelial cells through targeting SRF. *Int J Clin Exp Pathol*; 9(3):3357–3364.
64. Han S, Zhu J, Zhang Y. miR-144 Potentially Suppresses Proliferation and Migration of Ovarian Cancer Cells by Targeting RUNX1. *Medical science monitor basic research*. 2018 02; 24:40–46. <https://doi.org/10.12659/msmbr.907333> PMID: 29445078
65. Li J, Zhao Y, Lu Y, Ritchie W, Grau G, Vadas MA, et al. The Poly-cistronic miR-23-27–24 Complexes Target Endothelial Cell Junctions: Differential Functional and Molecular Effects of miR-23a and miR-23b. *Molecular Therapy—Nucleic Acids*. 2016; 5:e354. <https://doi.org/10.1038/mtna.2016.62> PMID: 27741223
66. Wu XD, Guo T, Liu L, Wang C, Zhang K, Liu HQ, et al. MiR-23a targets RUNX2 and suppresses ginseoside Rg1-induced angiogenesis in endothelial cells. *Oncotarget*. 2017; 8(35):58072–58085. <https://doi.org/10.18632/oncotarget.19489> PMID: 28938538
67. Zhu S, Pan W, Song X, Liu Y, Shao X, Tang Y, et al. The microRNA miR-23b suppresses IL-17-associated autoimmune inflammation by targeting TAB2, TAB3 and IKK-. *Nature Medicine*. 2012; 18(7):1077–1086. <https://doi.org/10.1038/nm.2815> PMID: 22660635
68. Reitsma S, Slaaf DW, Vink H, Zandvoort MAMJ, Egbrink MGA. The endothelial glycocalyx: composition, functions, and visualization. *European journal of physiology*. 2007; 454(3):345–359. <https://doi.org/10.1007/s00424-007-0212-8> PMID: 17256154

69. Zolla V, Nizamutdinova IT, Scharf B, Clement CC, Maejima D, Aki T, et al. Aging-related anatomical and biochemical changes in lymphatic collectors impair lymph transport, fluid homeostasis, and pathogen clearance. *Aging cell*. 2015; 14(4):582–594. <https://doi.org/10.1111/ace1.12330> PMID: 25982749
70. Chakraborty S, Zawieja SD, Wang W, Lee Y, Wang YJ, von der Weid P, et al. Lipopolysaccharide modulates neutrophil recruitment and macrophage polarization on lymphatic vessels and impairs lymphatic function in rat mesentery. *American journal of physiology. Heart and circulatory physiology*. 2015; 309(12):H2042–H2057 <https://doi.org/10.1152/ajpheart.00467.2015> PMID: 26453331
71. Bridenbaugh EA, Wang W, Srimushnam M, Cromer WE, Zawieja SD, Schmidt SE, et al. An immunological fingerprint differentiates muscular lymphatics from arteries and veins. *Lymphatic research and biology*. 2013 09; 11(3):155–171. <https://doi.org/10.1089/lrb.2013.0023> PMID: 24044756
72. Hunter MC, Teixeira A, Halin C. T Cell Trafficking through Lymphatic Vessels. *Frontiers in Immunology*. 2016; 7:613. <https://doi.org/10.3389/fimmu.2016.00613> PMID: 28066423
73. Khan AA, Alsayh MA, Rahmani AH. Myeloperoxidase as an Active Disease Biomarker: Recent Biochemical and Pathological Perspectives. *Medical sciences (Basel, Switzerland)*. 2018 04; 6(2):33.
74. Castillo-Tong DC, Pils D, Heinze G, Braicu I, Sehoul J, Reinhaller A, et al. Association of myeloperoxidase with ovarian cancer. *Tumour biology: the journal of the International Society for Oncodevelopmental Biology and Medicine*. 2014 01; 35(1):141–148.
75. Klinke A, Nussbaum C, Kubala L, Friedrichs K, Rudolph TK, Rudolph V, et al. Myeloperoxidase attracts neutrophils by physical forces. *Blood*. 2011; 117:1350–1355. <https://doi.org/10.1182/blood-2010-05-284513> PMID: 20980678
76. Tirupathi C, Naqvi T, Wu Y, Vogel SM, Minshall RD, Malik AB. Albumin mediates the transcytosis of myeloperoxidase by means of caveolae in endothelial cells. *Proceedings of the National Academy of Sciences of the United States of America*. 2004 05; 101(20):7699–7704. <https://doi.org/10.1073/pnas.0401712101> PMID: 15136724